Waveguide Side-Wall Coupling for RF Guns *

Leon C.-L. Lin, S. C. Chen, and J. S. Wurtele
Massachusetts Institute of Technology
Cambridge, MA 02139

Abstract

A theoretical analysis of the waveguide side-wall coupling of RF gun structures is presented. The analysis of this three dimensional problem yields an equivalent circuit whose elements are either directly calculated from the frequency and geometry of the gun, or are inferred from the two dimensional numerical solver URMEL. Good agreement between experiment and theory is seen in cold tests of our 17GHz $1\frac{1}{2}$- cell RF gun.

1 INTRODUCTION

Photocathode RF guns are a promising source of high brightness electron beams for free electron lasers and future linear colliders. Among existing RF gun systems, the $1\frac{1}{2}$- cell RF cavity design with a waveguide side-wall coupling scheme, as shown in Fig. 1, is most widely used [1, 2, 3]. Most experiments have been conducted at an RF frequency of 2.856GHz. However, until now there has been no solid theoretical understanding of this coupling. Such understanding is important if guns are to be scaled to the high RF frequencies under consideration for future linear colliders and compact high gradient accelerators. The difficulty in developing such a theory is that the complicated geometry, which includes a combination of a cylindrically symmetric $1\frac{1}{2}$- cell cavity with a rectangular waveguide plus two symmetry-breaking apertures, is not readily amenable to analytical methods.

We present a theoretical study of the waveguide side-wall coupling for the $1\frac{1}{2}$- cell RF gun cavity, and a detailed comparison with experimental measurements. Our method consists of the following: 1. The problem is initially simplified by ignoring the iris, exit hole, and ohmic loss. 2. Each coupling aperture is represented by a three-dimensional dipole vector. 3. The two dipole vectors are solved for self-consistently using the small aperture approximation and appropriate Green's functions. 4. The dipole radiation is used to calculate the reflection and transmission coefficients. From these coefficient an impedance and equivalent circuit are derived. 5. The iris, exit hole, and ohmic loss are included by introducing additional circuit elements. Details will be published elsewhere [6].
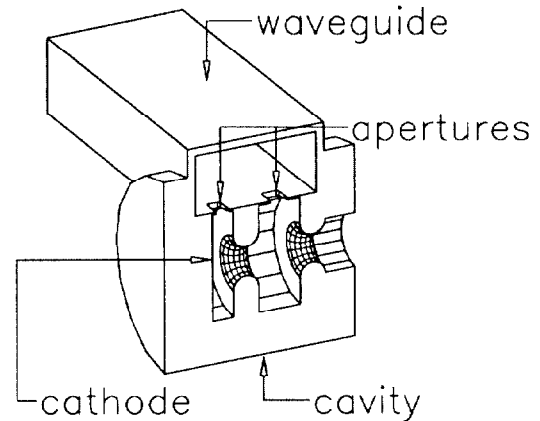
Figure 1: A cross section view of a $1\frac{1}{2}$- cell RF cavity coupled to a rectangular waveguide via two apertures in the side-wall.

2 CONSTRUCTION OF THE EQUIVALENT CIRCUIT

Consider the waveguide side-wall coupling problem shown in Fig. 1. The RF energy is coupled into the cavity through two apertures which are assumed to be small compared to the wavelength of the incident RF field. Let $i = 1, 2$ refer to these two apertures. The effects of a small aperture can be represented [4] by a dipole vector which consists of three components: an electrical component normal to the side-wall, and two tangential magnetic components. The dipole vector d_i at each aperture is related to a field vector F_i, whose components are the normal electric and two tangential magnetic field components. From the quasi-static solution of the wave equation it can be shown that

$$\begin{bmatrix} d_1 \\ d_2 \end{bmatrix} = \begin{bmatrix} \bar{\alpha}_1 & \bar{O} \\ \bar{O} & \bar{\alpha}_2 \end{bmatrix} \begin{bmatrix} F_1 \\ F_2 \end{bmatrix}, \qquad (1)$$

or simply $d = \bar{\alpha} \cdot F$. Here, $\bar{\alpha}_i$ is the aperture's polarizability tensor, readily given in terms of geometry [5]. To obtain a self-consistent, and thus a physically meaningful solution, one needs to include both the incident and the radiated fields. The total field at the aperture should thus be of the form $F = F^{inc} + F^g + F^c$, where F^{inc} denotes the incident field, and F^g (F^c) denotes the total field radiated by d on the waveguide side (cavity side) of the aperture.

Since this is a linear system, there exist reaction tensors $\bar{\chi}^g$ and $\bar{\chi}^c$ such that $F^{g,c} = \bar{\chi}^{g,c} \cdot d$. Thus the dipole vector d can be written in terms of the incident field F^{inc}

as

$$d = [\bar{\delta} - \bar{\alpha} \cdot (\bar{\chi}^g + \bar{\chi}^c)]^{-1} \cdot \bar{\alpha} \cdot F^{inc}, \qquad (2)$$

where $\bar{\delta}$ is the identity tensor. The coupling problem is thus determined by d, which depends on the reaction tensors for the waveguide and the cavity. These tensors are readily obtained from the Green's functions of the waveguide and pillbox cavities [6].

A two-port network, characterized by a two-by-two scattering matrix $\bar{S}$, gives physical insight into the coupling. The matrix $\bar{S}$ is related to its impedance matrix by

$$\bar{Z} = Z_0(\bar{\delta} - \bar{S})^{-1} \cdot (\bar{\delta} + \bar{S}), \qquad (3)$$

where Z_0 is the waveguide characteristic impedance. From the Green's function for waveguide, we calculate the radiated fields and then obtain the reflection coefficient S_{11} and the transmission coefficient S_{21}

$$S_{11} = \frac{j\beta}{2} f^+ \cdot [\bar{\delta} - \bar{\alpha} \cdot (\bar{\chi}^g + \bar{\chi}^c)]^{-1} \cdot \bar{\alpha} \cdot f^+, \qquad (4)$$

$$S_{21} = 1 + \frac{j\beta}{2} f^- \cdot [\bar{\delta} - \bar{\alpha} \cdot (\bar{\chi}^g + \bar{\chi}^c)]^{-1} \cdot \bar{\alpha} \cdot f^+, (5)$$

where $\beta = \sqrt{(\omega/c)^2 - k_c^2}$ (k_c is the cutoff wavenumber) and the elements $f^{\pm}$ are given in [6]. In practice, the waveguide is shorted at a quarter-wave distance from the apertures. This maximizes the incident fields on the apertures. In this case, port two is open and the two-port network becomes a one-port network with an impedance Z_{11}. Inserting Eqs. 4 and 5 into Eq. 3 yields an expression for the impedance Z_{11}. The result is the compact expression:

$$Z_{11} = jX_x + 1/jB_y + 1/Y_{1z} + 1/Y_{2z} \qquad (6)$$

where $Y_{iz} = jX_{iz} + n_i^2/(j\omega C_i + 1/j\omega L_i)$. Each element is rigorously given in terms of frequency and geometry [6].

The iris can be represented by a mutual inductor M and a capacitor C_t, the exit hole can be represented by a capacitor C_e, and ohmic loss can be represented by conductances G_1 and G_2. Their numerical values can be obtained from the numerical solver URMEL [6]. This yields the equivalent network shown in Fig. 2. In this equivalent network, we have introduced an additional capacitor C_t' to represent the tuner used to change the frequency of the first cell in our experimental apparatus.

In Figure 2, L_1-C_1 (L_2-C_2) represent the oscillation of the first (second) cell, M represents the coupling due to the iris, C_t represents the tuning due to the iris, C_e represents the tuning due to the exit hole in the second cell, C_t' represents the tuning due to the tuner in the first cell, G_1 and G_2 models ohmic losses in two cells, the two transformers $n_1 : 1$ and $n_2 : 1$ represent the impedance transforming features of the waveguide-cavity junction, and jX_x, jB_y, jX_{1z}, and jX_{2z} represent the waveguide-cavity coupling.

3   COUPLED OSCILLATORS MODEL

In our gun, the coupling is primarily through the z component of the dipole. This implies jX_x and jB_y are negligible. Near resonance we obtain, from the equivalent circuit,

two driven coupled oscillators equations:

$$\begin{bmatrix} j(\omega - \omega_1' - j\tau_1) & -\kappa \\ -\kappa & j(\omega - \omega_2' - j\tau_2) \end{bmatrix} \begin{bmatrix} u_1 \\ u_2 \end{bmatrix} = \begin{bmatrix} q_1 \\ q_2 \end{bmatrix}.$$

Here, u_i is the normalized accelerating field amplitude, ω_i' the resonant frequency, τ_i the loss factor (which is related to the cavity Q-factor), q_i the driving force, and κ the coupling coefficient.

The eigenvalues and eigenvectors of the coupled oscillators are

$$\omega_{\pm}' = \frac{\Omega_1 + \Omega_2}{2} \pm \sqrt{(\frac{\Omega_1 - \Omega_2}{2})^2 - \kappa^2},$$

$$\bar{U} = [\begin{array}{cc} u_+ & u_- \end{array}] = \begin{bmatrix} \cos\theta & -\sin\theta \\ \sin\theta & \cos\theta \end{bmatrix},$$

where $\Omega_i = \omega_i' + j\tau_i$ and

$$\theta = \tan^{-1}\frac{j(\omega_+' - \Omega_1)}{\kappa}. \qquad (7)$$

The eigenmodes u_+ and u_- are the π- mode and the 0-mode for the waveguide side-wall coupled $1\frac{1}{2}$ cell RF cavity, respectively. The angle θ is the mode mixing angle. We can represent the response u as a linear combination of u_+ and u_-:

$$u = [\frac{c_+}{j(\omega - \omega_+')}u_+ + \frac{c_-}{j(\omega - \omega_-')}u_-] \qquad (8)$$

where

$$c_+ = q_1 \cos\theta + q_2 \sin\theta \qquad (9)$$

$$c_- = -q_1 \sin\theta + q_2 \cos\theta. \qquad (10)$$

Note that c_+ and c_- represent the magnitude of the π-mode and the 0- mode, respectively. If c_+ is much greater than c_-, then the π- mode has been selectively excited.

In general, it is likely that the cavity will be in the weak-coupling region ($\theta \sim 0$ or $\theta \sim \pi/2$) before tuning. In this case, both the 0- mode and the π- mode are excited with comparable magnitudes (since $q_1 \sim q_2$). To excite a pure π- mode, we tune the cavity until strong-coupling ($\theta \sim \pi/4$) is reached. Then, since $c_- \propto (q_2 - q_1) \sim 0$, the 0- mode is suppressed.

4   COMPARISON BETWEEN EXPERIMENT AND THEORY

In this section, the theoretical and measured values of the reflection coefficient (S_{11}) for a 17GHz RF gun [3] are presented. The data was obtained using a HP8510 network analyzer. In Fig. 3, theoretical and measured values of the reflection coefficient S_{11} are plotted as a function of frequency for an initially untuned gun. Without tuning the system is in the weak coupling region; in our case the first cell has the lower resonant frequency. The two apertures are commensurate in size and consequently $q_1 \sim q_2$. Therefore, one observes two distinct resonances with comparable magnitude.
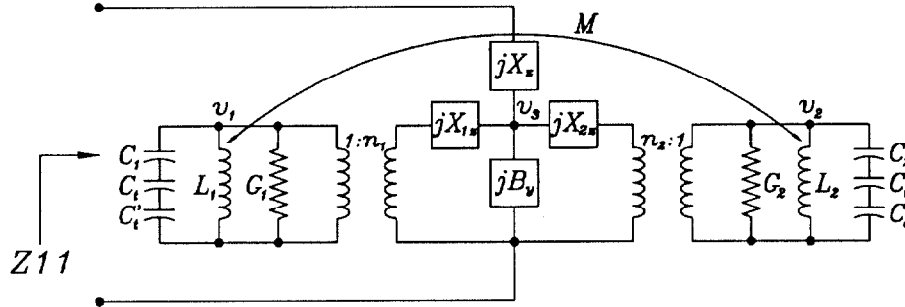
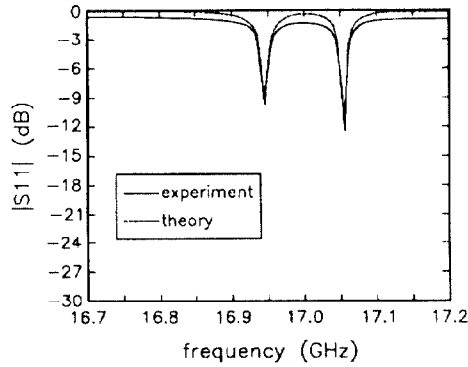Figure 2: An equivalent network for the complete wave-guide side-wall coupled $1\frac{1}{2}$-cell cavity system.

Figure 3: $|S_{11}|$ of the waveguide side-wall coupled $1\frac{1}{2}$- cell cavity as a function of frequency when the cavity is untuned.
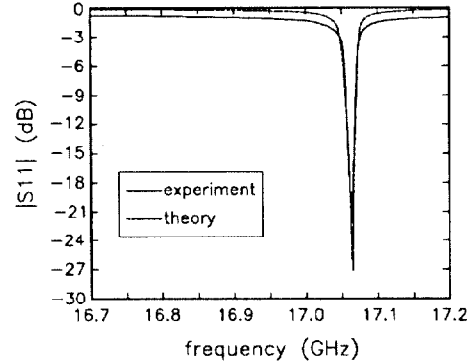

Figure 4: S_{11} of the waveguide side-wall coupled $1\frac{1}{2}$- cell cavity as a function of frequency when the cavity is properly tuned.

We next study the frequency dependence of S_{11} for different values of the tuning of the first cell. As we tune the first cell, the resonant frequency of the first cell (ω'_1) becomes larger and thus closer to that of the second cell (ω'_2). In addition, the coupling coefficient κ and driving forces q_1 and q_2 are insensitive to the tuning. Therefore, the coupling becomes stronger. Finally, two resonances become undistinguishable when the difference in frequency is greater than the bandwidth, as shown in Fig. 4. In these figures, the theoretical predictions agree very well with measurement. Note that the baseline of the reflectivity is 0dB for the theory as opposed to $-.8$dB for the data, because the insertion loss of the waveguide is not included in the theory.

5 CONCLUSION

We have constructed an equivalent network representation for the waveguide side-wall coupled $1\frac{1}{2}$- cell RF cavity. The coupling between the rectangular waveguide and the cylindrical $1\frac{1}{2}$- cell cavity (without the iris, the exit hole, and ohmic losses) has been studied using the small aperture approximation and rigorously represented by an equivalent network, in which all circuit elements are derived from first principles. The iris, the exit hole, and ohmic loss have been modeled by introducing appropriate circuit elements obtained from the numerical field solver URMEL. The resultant equivalent circuit has been analyzed and well ap-

proximated by two driven coupled oscillators. We have shown that with proper tuning the waveguide side-wall coupling scheme can selectively excite a linear combination of π- and 0- modes so as to optimize the RF gun performance. Experimental measurements of the frequency response of the waveguide side-wall coupled cavity under different tuning have been shown to be in good agreement with our theory.

6 REFERENCES

[1] K. Batchlor et al., "Design and Modelling of a 5MeV Radio Frequency Electron Gun", BNL-41766, 1988.

[2] F. Aghamir et at., "SATURNUS: The UCLA High Gain Infrared FEL Project," UCLA-CAA0068-9/90, 1990.

[3] S. C. Chen et al., "High Gradient Acceleration in a 17GHz Photocathode RF Gun," AIP Conference Proc. 279, pp. 694-705, 1993.

[4] H. A. Bethe, "Theory of Diffraction by Small Holes," Phys. Rev., vol. 66, pp. 163-182, 1944.

[5] R. E. Collin, Field Theory of Guided Waves, New York: IEEE Press, pp. 499-511, 1991.

[6] L. C.-L. Lin, S. C. Chen, and J. S. Wurtele, "An Equivalent Network Analysis of Waveguide Side-Wall Coupled RF Gun Structures," in preparation, to be published.